

## Solid-State Characterization of 2-[(2,6-Dichlorophenyl)amino]-Benzaldehyde: An Experimental and Theoretical Investigation

Peng Chen,<sup>a,†</sup> Yuanyuan Jin,<sup>b,†</sup> Panpan Zhou,<sup>c</sup> Sean Parkin,<sup>d</sup> Zhifei Zhang<sup>e,\*</sup> and Sihui Long<sup>a,\*</sup>

<sup>a</sup>Key Laboratory for Green Chemical Process of Ministry of Education, School of Chemical Engineering and Pharmacy, Wuhan Institute of Technology, Wuhan, Hubei, China

<sup>b</sup>Institute of Medicinal Biotechnology, Chinese Academy of Medical Sciences, Beijing, China

<sup>c</sup>Department of Chemistry, Lanzhou University, Lanzhou, Gansu, China

<sup>d</sup>Department of Chemistry, University of Kentucky, Lexington, KY, USA

<sup>e</sup>School of Pharmacy, North China University of Science and Technology, Tangshan, China

(Received: December 13, 2016; Accepted: February 22, 2017; Published Online: March 27, 2017; DOI: 10.1002/jccs.201600848)

The solid-state properties of 2-[(2,6-dichlorophenyl)amino]-benzaldehyde (DCABA) were investigated. Unlike its precursor diclofenac acid, for which three polymorphs are currently known, only one crystalline form of DCABA was found. It was further characterized by other spectroscopic and spectrometric methods including IR, Raman, and UV–vis spectroscopy and powder X-ray diffraction (PXRD). The thermal behavior of the crystalline form was studied by differential scanning calorimetry (DSC). Theoretical studies, including Hirshfeld surface analysis and conformational energy searches, were performed to provide insight into the factors contributing to the stability of the crystal and to assess the possibility of additional polymorphs. The full characterization of this compound can help fast and accurate identification of DCABA both in dosage forms and in the environment.

**Keywords:** 2-[(2,6-Dichlorophenyl)amino]-benzaldehyde; Crystal structure; Spectroscopy; Conformational search; Hirshfeld surface analysis.

### INTRODUCTION

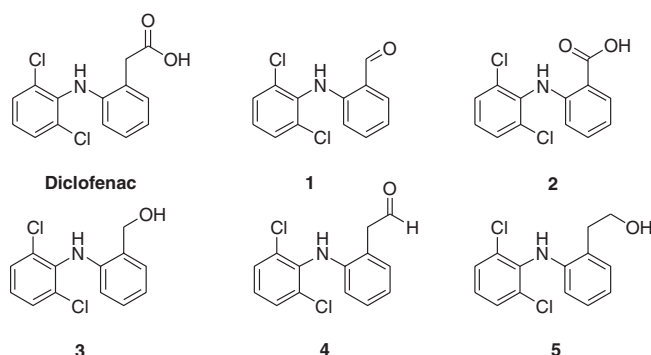
The stability of drugs is of utmost importance, as the products of their metabolism and decomposition may cause adverse effects and become potential environmental contaminants. Less commonly, they might also lead to new drugs. Thus the metabolic products and other derivatives of pharmaceuticals have been receiving increasing scientific and public attention.<sup>1,2</sup> Diclofenac acid (DCF; 2-[(2,6-dichlorophenyl)amino]benzeneacetic acid) is one of the most commercially successful nonsteroidal anti-inflammatory drugs (NSAIDs). As with all NSAIDs, DCF exerts anti-inflammatory, analgesic, and anti-pyretic actions via inhibition of the cyclooxygenase I (COX I) and

cyclooxygenase II (COX II) enzymes.<sup>3</sup> Physiologically, DCF is known to metabolize in the liver through decarboxylation, hydroxylation, oxidation, etc. In the environment, DCF undergoes phototransformation to generate a variety of derivatives, including 2-[(2,6-dichlorophenyl)amino]-benzaldehyde (DCABA) (Scheme 1).<sup>4,5</sup>

DCABA is likely produced by decarboxylation followed by oxidation of DCF.<sup>6</sup> Because of the presence of the aldehyde functional group, which can participate in a variety of reactions such as reduction, oxidation, and nucleophilic addition, DCABA should be chemically active and might cause unwanted side effects on both the human body and the environment. Thus a thorough characterization of the compound, particularly the thermal and spectral characteristics, should aid the identification of the impurity within accelerated stability testing of final dosage forms.

<sup>†</sup> Peng Chen and Yuanyuan Jin contributed equally to this work.

\*Corresponding authors. Email: zhangzhifeifei7208@163.com; Sihuilong@wit.edu.cn, longsihui@yahoo.com



Scheme 1. Structure of DCABA and related compounds.

We are interested in the solid-state properties of pharmaceuticals as well as their derivatives. Three polymorphic forms of diclofenac acid are reported in the literature. Two forms, referred to as HD1 (space group  $P2_1/c$ ) and HD2 (space group  $C2/c$ ) are monoclinic.<sup>7</sup> In both forms, the molecules are linked through the common carboxylic acid dimer motif ( $R_2^2(8)$ ) by the graph set concept<sup>8–10</sup>. The difference between them lies in the relative positions of the carboxylic acid group, the aromatic ring it is attached to, and the hydrogen bonding parameters in the dimers. A third polymorph is orthorhombic (HD3, space group  $Pcan$ ), in which no intermolecular hydrogen bond is observed. Yet the quality of the diffraction data is poor likely due to the small size of the crystal (crystal size:  $0.13 \times 0.06 \times 0.02$  mm; final  $R$ -index = 0.1360).<sup>11</sup> In this study, we investigate the structure of DCABA through a combination of experimental and theoretical approaches including single-crystal X-ray diffraction, powder X-ray diffraction (PXRD), DSC, IR, Raman, UV–vis spectroscopy, conformational energy searches, and Hirshfeld surface studies. A comparison of DCABA and the other structurally related compounds 2-[(2,6-dichlorophenyl)amino]benzoic acid (**2**), 2-[(2,6-dichlorophenyl)amino]benzenemethanol (**3**), 2-[(2,6-dichlorophenyl)amino]benzenealdehyde (**4**), and 2-[(2,6-dichlorophenyl)amino]benzeneethanol (**5**) is also attempted.

## RESULTS AND DISCUSSION

### Crystal structure

Crystal structure is the most definitive identification of a given compound. Although DCABA is known to be a derivative of DCF, no crystal structure has thus

Table 1. Crystal growth of 2-[(2,6-dichlorophenyl)amino]benzaldehyde

Solvent	Growth condition	Form
Methanol	Slow evaporation	I
Ethanol	Slow evaporation	I
Chloroform	Slow evaporation	I
Acetone	Slow evaporation	I
Ethyl acetate	Slow evaporation	I
Dichloromethane	Slow evaporation	I
Tetrahydrofuran	Slow evaporation	I
Dimethylsulfoxide	Slow evaporation	I
Acetonitrile	Slow evaporation	I

far been reported. In this study, we obtained the first crystal structure of DCABA. Crystals obtained from a variety of solvents (Table 1) grow as yellow plates (Figure 1), and are monoclinic in space group  $P2_1/c$  ( $Z = 4$ ). Crystallographic data are given in Table 2 (for the complete CIF file, see the Supporting Information).

In the crystal, the molecule has a twisted conformation with a dihedral angle of  $64.5(1)^\circ$  between the two aromatic rings. There is an intramolecular hydrogen bond between the amino group NH and the carbonyl of the aldehyde (S6 in the graph set notation<sup>8–10</sup>) with a bond distance of 2.06 Å and bond angle of  $131.0^\circ$  (Figure 1(b)). In addition, a nonclassical intermolecular hydrogen bond  $sp^2C-H \cdots Cl$  with bond parameters of 2.84 Å and  $172.2^\circ$  is observed. In contrast, the structure of DCF is based on the acid–acid dimer as mentioned previously. An intramolecular hydrogen bond between NH and  $O=C$  also exists, but no  $sp^2C-H \cdots Cl$  hydrogen bond is obvious. Structures are not available for other related compounds except for compound **5**, in which only an intramolecular  $N-H \cdots OH$  hydrogen bond (S7) exists and no halogen bond or  $sp^2C-H \cdots Cl$  hydrogen bond is observed.<sup>12</sup>

### Thermal properties

Thermal properties such as melting point and potential phase transitions are important aspects of most solid compounds. In this work, DSC was carried out to investigate the thermal properties of the crystals (Figure 2). There is only one thermal event, which corresponds to the melting of the crystals, with an onset temperature of  $105^\circ\text{C}$ . No other peaks that could indicate solid–solid phase transitions were detected. In comparison, DCF has a much higher melting point

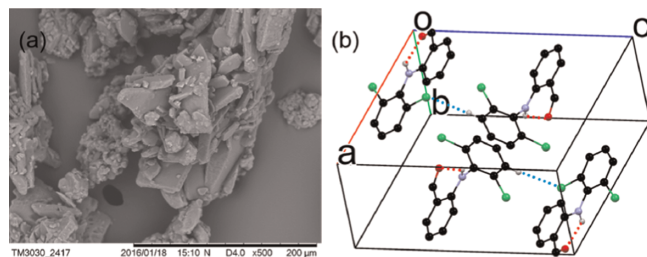


Fig. 1 (a) SEM image of 2-[(2,6-dichlorophenyl)amino]-benzaldehyde crystals. Scale bar 200  $\mu\text{m}$ . (b) Crystal packing of 2-[(2,6-dichlorophenyl)amino]-benzaldehyde (for clarity, hydrogens not involved in hydrogen bonding were omitted).

Table 2. Crystallographic data of 2-[(2,6-dichlorophenyl)amino]-benzaldehyde

	Compound
Formula	$\text{C}_{13}\text{H}_9\text{Cl}_2\text{NO}$
Formula weight	266.11
Crystal size (mm)	$0.25 \times 0.20 \times 0.12$
Crystal system	Monoclinic
Space group	$P21/c$
$a/\text{\AA}$	11.0800 (10)
$b/\text{\AA}$	8.1945 (7)
$c/\text{\AA}$	13.7224 (12)
$\alpha/^\circ$	90
$\beta/^\circ$	106.6900 (10)
$\gamma/^\circ$	90
$Z, Z'$	4, 1
$V/\text{\AA}^3$	1193.44 (18)
$D_{\text{calc}}/\text{g}\cdot\text{cm}^{-3}$	1.481
T/K	298 (2)
Abs. Coeff. ( $\text{mm}^{-1}$ )	0.524
$F(000)$	544
$\theta$ range( $^\circ$ )	1.92–27.00
Limiting indices	$-14 \leq h \leq 14$ $-10 \leq k \leq 4$ $-17 \leq l \leq 17$
Completeness to $2\theta$	99.5%
Unique reflections	2021
$R1[I > 2\sigma(I)]$	4.25
$wR^2$ (all data)	12.26

(156–158 $^\circ\text{C}$ ), which is attributed to the intermolecular acid–acid dimer in the solid state. Similarly, the high melting point (218–220 $^\circ\text{C}$ ) of compound **2** is also due to the strong intermolecular acid–acid hydrogen bond. In contrast, the melting points of the two alcohols, namely **3** and **5** (both close to 110 $^\circ\text{C}$ ), are just slightly

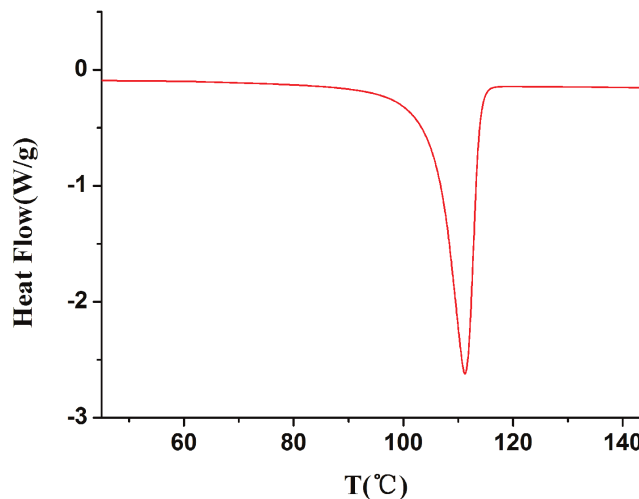


Fig. 2. DSC thermogram of 2-[(2,6-dichlorophenyl)amino]-benzaldehyde.

higher than that of DCABA, probably because of the lack of strong intermolecular interactions. For compound **4**, no related parameter has been reported.

#### Powder X-ray diffraction

PXRD enables fast identification of a solid sample when a single crystal is not available but the crystal structure is known. Figure 3 shows the room-temperature PXRD pattern of pulverized crystals, along with a pattern calculated from the single-crystal structure determined at 298 K. The near-perfect match between the experimental and calculated patterns indicates the identity and phase purity of the crystal form.

#### Spectroscopic characteristics

Spectroscopic methods, such as IR, Raman, and UV–vis, can provide structural information regarding the compounds under investigation in a convenient manner. The IR spectrum (Figure 4(a)) shows the characteristic peaks of DCABA: for example, N–H stretch at 3249  $\text{cm}^{-1}$ ,  $\text{sp}^2$  C–H stretch in the range of 3000–3100  $\text{cm}^{-1}$ , aldehyde C–H at 2848 and 2716  $\text{cm}^{-1}$ , aldehyde C = O stretch at 1660  $\text{cm}^{-1}$ , aromatic C = C stretch from 1605 to 1506  $\text{cm}^{-1}$ , C–N stretch at 1320  $\text{cm}^{-1}$ , and C–Cl stretch at around 750  $\text{cm}^{-1}$  (Table 3).

The Raman spectrum (Figure 4(b)) consists aromatic C–H stretch at 3072.5  $\text{cm}^{-1}$ , aldehyde C–H stretch at 2878.3  $\text{cm}^{-1}$ , C = O stretch at 1655.5  $\text{cm}^{-1}$ , N–H bending at 1582.1  $\text{cm}^{-1}$ , aromatic C = C stretch

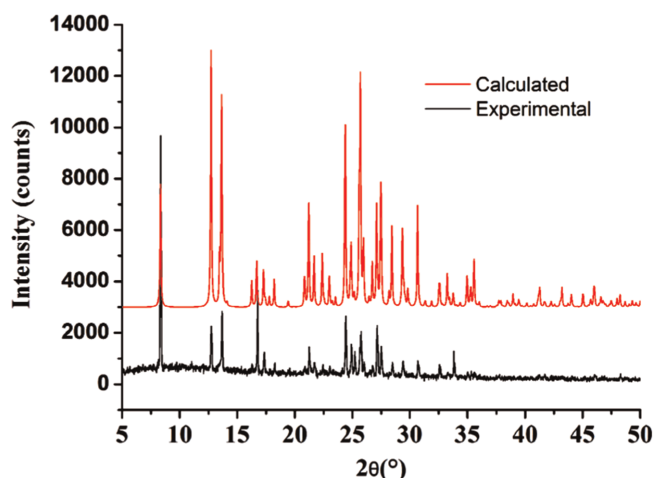


Fig. 3. Experimental and calculated powder X-ray diffraction patterns of 2-[(2,6-dichlorophenyl)amino]benzaldehyde.

at 1603.2, 1574.0, and 1557.1  $\text{cm}^{-1}$ , C–N stretch at 1323.9  $\text{cm}^{-1}$ , and C–Cl stretch at 713.1  $\text{cm}^{-1}$  (Table 3).

Interestingly, for the related compounds, no such spectroscopic characterization has been performed. But we can expect characteristic IR and Raman fingerprints for the specific functional groups such as carboxylic acid in DCF and **2** and hydroxyl group in **3** and **5**. The spectra for **4** could be expected to be nearly identical to that of DCABA.

DCABA is not soluble in apolar solvents, so the UV–vis spectra were measured in dichloromethane. Two peaks were observed in the UV–vis spectrum: one at  $\lambda_{\text{max}} = 368$  nm with a molar absorptivity of 4045.8 L/mol/cm, which can be attributed to  $n \rightarrow \pi^*$  excitation of the aldehyde functional group; and the other at  $\lambda_{\text{max}} = 280$  nm with a molar absorptivity of 3497.1 L/mol/cm, which results from a  $\pi \rightarrow \pi^*$  excitation of the benzaldehyde ring. The shoulder peak next to it may be from the excitation of the chlorinated aromatic ring. Experimental and calculated UV–vis spectra are very similar in peak appearance, but the wavelengths of individual peaks do not match exactly. This could be due to the solvent effect (Figure 5).

Still, no UV–vis study has been carried out for the related compounds. Because of the presence of various functional groups and the degree of conjugation between the two aromatic rings in different compounds, a characteristic UV–vis spectrum could be expected for the individual compounds.

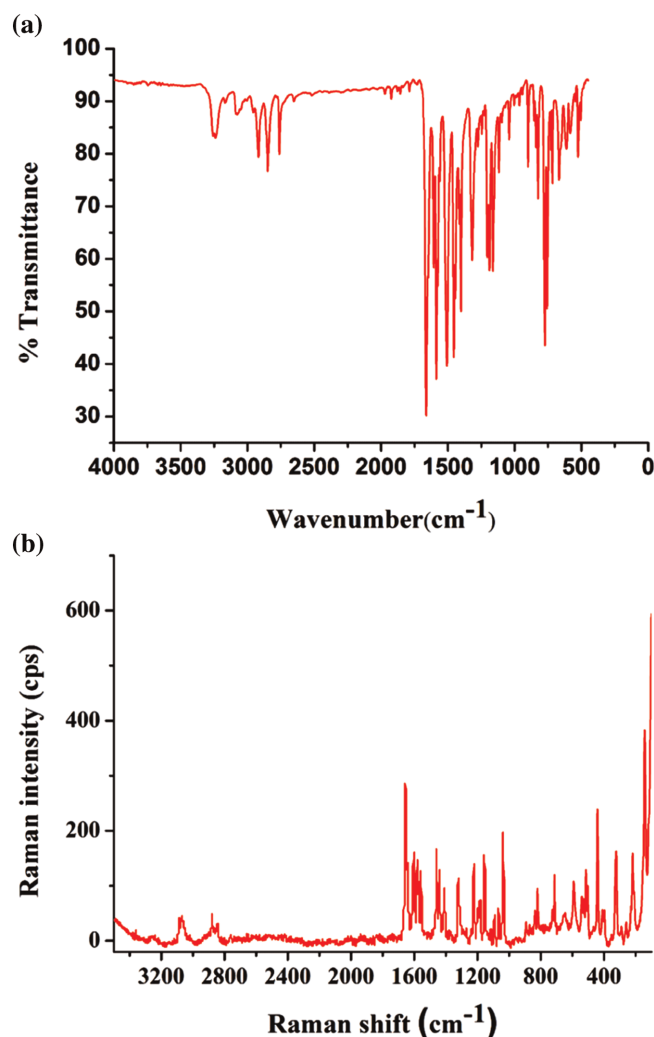


Fig. 4. (a) IR and (b) Raman spectrum of 2-[(2,6-dichlorophenyl)amino]benzaldehyde.

Structure of a compound determines its properties. Because of the lack of strong intermolecular interactions such as the classical hydrogen bonds between the molecules in the solid state, the melting point of DCABA is on par with that of the related alcohols (**3** and **5**), which also form only intramolecular hydrogen bonds, and much lower than the related carboxylic acid compounds DCF and **2**. The vibrational spectra such as IR and Raman, also reflect the effect of the intramolecular hydrogen bond between NH and O = C. For example, the N–H stretch is at a lower wavenumber at 3249  $\text{cm}^{-1}$ , and the aldehyde C = O stretch is at 1660  $\text{cm}^{-1}$ . The UV–vis spectrum is a reflection of the equilibrium of a variety of conformations in the solution rather than the locked

Table 3. Characteristic IR and Raman peaks of 2-[(2,6-dichlorophenyl)amino]-benzaldehyde

IR spectrum						
N–H stretch	Sp <sup>2</sup> C–H stretch	Aldehyde C–H stretch	Aldehyde C=O stretch	Aromatic C=C stretch	C–N stretch	C–Cl stretch
3249	3000 –3100	2848 2716	1660	From 1605 to 1506	1320	750
m	m	m	s	s	s	m
Raman spectrum						
Aromatic C–H stretch	Aldehyde C–H stretch	C=O stretch	N–H bend	Aromatic C=C stretch	C–N stretch	C–Cl stretch
3072.5	2878.3	1655.5	1582.1	1603.2 1574.0 1557.1	1323.9	713.1

conformer in the solid state, thus the correlation is decent.

### Computational Results

**Conformational search** To investigate the conformation in the crystal structures, the energy of a single DCABA molecule was evaluated as a function of the torsion angle  $\tau$  (Figure 6(a)) using the Gaussian 09 program.<sup>13</sup> The most stable conformer was identified, first, by comparing the optimized structures from various initial structures, and then with subsequent variation of the torsion angle with all bond lengths and bond angles fixed. Basis sets at the B3LYP/6-311G(d,p) and B3LYP/6-311++G(d,p) levels of theory were used for the structural optimization and conformational search, respectively.

The global minimum of  $\tau$  occurred at  $-72.5^\circ$ , which is close to the torsion angle observed in the crystal ( $-74.6^\circ$ ). Other than the global minimum, four local minima reside on the potential energy surface with  $\tau$  values at around  $-102^\circ$  (0.74 KJ/mol),  $80^\circ$  (0.73 KJ/mol),  $110^\circ$  (0.75 KJ/mol), and  $140^\circ$  (2.56 KJ/mol) (Figure 6(b)). These alternative conformers are theoretically accessible since the energy barrier between the global minimum and the local minima is not higher than 3 KJ/mol.

**Hirshfeld surface analysis** To further understand the relative contributions to intermolecular interactions by various molecular contacts in the crystal, Hirshfeld surface analysis<sup>14,15</sup> was performed with CrystalExplorer (Version 3.1)<sup>16</sup>; the result is shown in Figure 7. From the 2D fingerprint plot, we can see that all the contacts

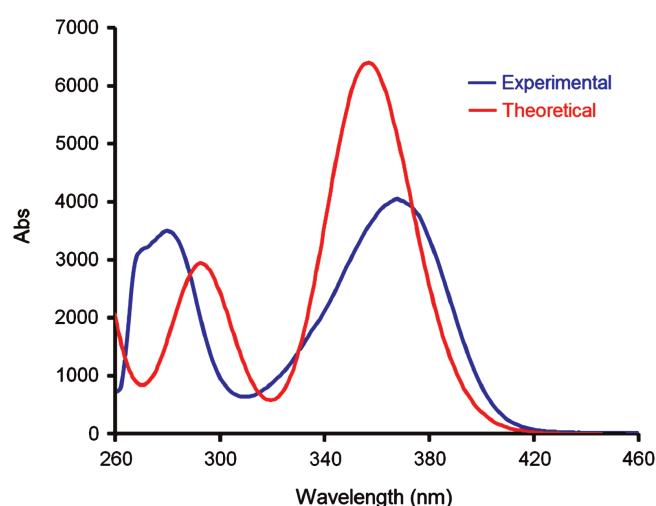


Fig. 5. Calculated and experimental UV-vis spectrum of 2-[(2,6-dichlorophenyl)amino]-benzaldehyde in dichloromethane.

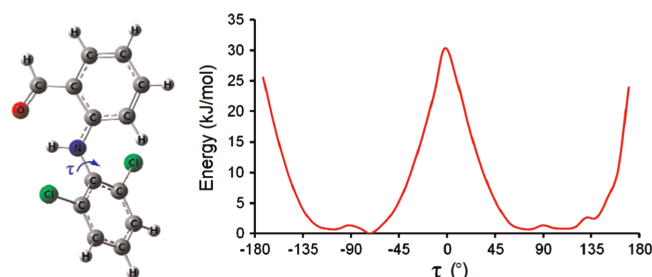


Fig. 6. Conformational search of  $\tau$  of a single 2-[(2,6-dichlorophenyl)amino]-benzaldehyde molecule.

are within the range of  $1.0 < d_e, d_i < 2.6$ . It is evident that hydrogen–hydrogen contacts contribute to about 33% of the Hirshfeld surface since hydrogens are the

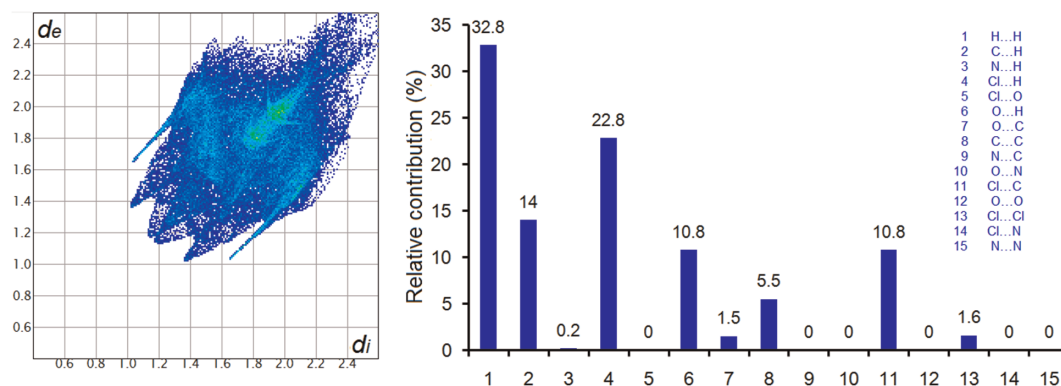


Fig. 7. 2D fingerprint plot (on the left) for 2-[(2,6-dichlorophenyl)amino]-benzaldehyde and relative contribution to the Hirshfeld surface (histograms on the right) for the various intermolecular contacts for the molecules in the crystal.

peripheral atoms, and the Cl...H contacts predominate over other interactions. Other significant interactions include C...H (14%), O...H, and Cl...C contacts with similar contributions (~11%). The contribution by C...C contacts is 5.5%, which is possibly due to  $\pi$ - $\pi$  interactions between aromatic rings. Moreover, Cl...Cl contacts contribute ~1.6% to the overall interactions. The analysis thus indicates that the crystal structure is maintained mainly by hydrogen bonding and facilitated by van der Waals interactions.

## EXPERIMENTAL

### Materials

All solvents and reagents were purchased from commercial sources (Sinopharm Chemical Reagent Co., Ltd., Shanghai, China) and used as received. 2-[(2,6-Dichlorophenyl)amino]-benzaldehyde was obtained upon purification of DCF by HPLC in our own laboratory.

### Crystal Growth

The crystal growth by slow evaporation was carried out for polymorph screening of 2-[(2,6-dichlorophenyl)amino]-benzaldehyde.<sup>17,18</sup> The compound was dissolved in different solvents (methanol, ethanol, chloroform, acetone, ethyl acetate, dichloromethane, tetrahydrofuran, dimethylsulfoxide, and acetonitrile). For example, 100 mg of 2-[(2,6-dichlorophenyl)amino]-benzaldehyde was added to 10 mL HPLC-grade methanol. The mixture was stirred overnight and the remaining solid was removed by pipette filtration. A vial containing the solution was covered with

perforated parafilm and left undisturbed. Slow evaporation led to single crystals in about a week (pictures were taken with a TM3030 scanning electron microscope, Hitachi, Japan). All crystallization experiments were conducted in the open air, and each was repeated multiple times. The identity of the crystals was confirmed by PXRD and, when high-quality single crystals were obtained, by single-crystal X-ray diffraction. All experiments generated the same solvent-free crystal form.

### Crystal Structure Determination

Crystal structure of 2-[(2,6-dichlorophenyl)amino]-benzaldehyde was determined by single-crystal X-ray diffraction. Data collection was carried out at 298 K on a Bruker SMART APEX CCD (Bruker, Germany) area detector diffractometer using Mo K $\alpha$  radiation ( $\lambda = 0.71073 \text{ \AA}$ ) using  $\omega$  and  $\phi$  scans. Integration of the raw diffraction frames was performed using the program SAINT. The structure was solved by direct methods using the SHELXS program of the SHELXTL package and refined by full-matrix least-squares methods with SHELXL.<sup>19,20</sup> All non-hydrogen atoms were refined with anisotropic displacement parameters. All hydrogen atoms were placed in calculated positions and refined with isotropic displacement parameters tied to the parent atom.

PXRD analysis was performed with a Bruker D8 ADVANCE X-ray diffractometer (Bruker, Germany) with Ni-filtered Cu K $\alpha$  radiation (40 kV, 30 mA). The data were collected over a  $2\theta$  range of  $5.0^\circ$ – $50.0^\circ$  at a scan rate of  $1.0^\circ/\text{min}$ .

### Thermal Analysis

The phase behavior of the solid form was investigated by differential scanning calorimetry (DSC) with an SII DSC 6220 (SEIKO, Japan) apparatus. Tzero<sup>®</sup> pans and aluminum hermetic lids were used, and a heating rate of 10°C/min was applied. For the measurement, a few milligrams of the sample was placed in an aluminum pan with a pin hole in the lid, and heated under nitrogen flow.

### Spectroscopic studies

**Vibrational spectroscopy (IR and Raman)** IR spectra were recorded with the sample dispersed in KBr pellets using a Perkin-Elmer FT-IR spectrometer (Perkin Elmer, USA), while Raman spectra were recorded on samples compressed in a gold-coated sample holder using a Thermo Electron DXR Laser Confocal Microscopy Raman Spectrometer (Thermo Fisher, USA).

**UV-vis** UV-vis spectra were recorded using a Lambda 750 UV/vis/NIR spectrophotometer (Perkin Elmer) from solutions (in dichloromethane) contained in quartz cuvettes.

### Computational details

For conformational energy searches, the energies of an isolated DCABA single molecule with different conformations were evaluated using Gaussian 09 program (Gaussian, Inc., Wallingford, CT).<sup>13</sup> Molecules from various initial conformations were optimized at the B3LYP/6-311++G(d,p) level of theory to identify the most stable conformation, which was then used for the torsion angle scanning with all bond lengths and bond angles fixed. The same method was used for the conformational search due to its high accuracy.<sup>21</sup> Frequency calculations were performed for all optimized structures to identify energy minima (no imaginary frequency). UV spectrum was calculated based on the optimized geometry of DCABA. All calculations were conducted on a Linux cluster.

### CONCLUSIONS

The solid-state properties of 2-[(2,6-dichlorophenyl)amino]-benzaldehyde, an impurity in and a metabolite of the classic NSAID diclofenac acid, were investigated. One crystal form was obtained for the first time by crystallization from a variety of solvents, and it was characterized by a variety of spectroscopic

methods. The crystal structure is stabilized by intramolecular hydrogen bonding between the aldehyde oxygen and secondary amino group bridging the two aromatic rings and a nonclassical  $sp^2C-H \cdots Cl$  hydrogen bond. Thermal behavior indicated that this solid form does not undergo phase transition to convert into new forms. One likely reason for this is that the conformation in the crystal is very much the same as the optimized conformation for an isolated molecule. There would be little driving force for any sort of rearrangement. PXRD revealed the phase purity of the harvested crystals, thus excluding the existence of other forms in the sample. Hirshfeld surface analysis provided in-depth information regarding other factors contributing to the overall stability of the crystal form. The lack of polymorphs of DCABA is likely due to the steric hindrance caused by the two chlorines at the *ortho* positions of the amino group, which prohibits the free rotation along the N–C bond. But more polymorphs are still possible as suggested by the conformational scan, since multiple local minima were observed. The full characterization of this compound could help fast and accurate identification of DCABA both in dosage forms and in the environment.

### ACKNOWLEDGMENTS

SL thanks the Natural Science Foundation of Hubei Province (2014CFB787) and the Innovation Fund from Wuhan Institute of Technology (CX2014002) for financial support. PPZ acknowledges financial support by the National Natural Science Foundation of China (Grant No. 21403097) and the Fundamental Research Funds for the Central Universities (lzujbky-2014-182).

### REFERENCES

1. P. E. Stackelberg, E. T. Furlong, M. T. Meyer, S. D. Zaugg, A. K. Henderson, D. B. Reissman, *Sci. Total Environ.* **2004**, 329, 99.
2. L. H. Santos, A. N. Araujo, A. Fachini, A. Pena, C. Delerue-Matos, M. C. Montenegro, *J. Hazard. Mater.* **2010**, 175, 45.
3. R. Pireddu, C. Sinico, G. Ennas, F. Marongiu, R. Muzzalupo, F. Lai, A. M. Fadda, *Eur. J. Pharm. Sci.* **2015**, 77, 208.
4. A. Aguera, L. A. Perez Estrada, I. Ferrer, E. M. Thurman, S. Malato, A. R. Fernandez-Alba, *J. Mass Spectrom.* **2005**, 40, 908.

5. B. Cwiertnia, T. Hladon, M. Stobiecki, *J. Pharm. Pharmacol.* **1999**, *51*, 1213.
6. C. M. B. Neves, M. M. Q. Simoes, M. R. M. Domingues, I. C. M. S. Santos, M. G. P. M. S. Neves, F. A. Almeida Paz, A. M. S. Silva, J. A. S. Cavaleiro, *RSC Adv.* **2012**, *2*, 7427.
7. C. Castellari, S. Ottani, *Acta Cryst* **1997**, *C53*, 794.
8. J. Bernstein, R. E. Davis, L. Shimoni, N. L. Chang, *Angew. Chem. Int. Ed.* **1995**, *34*, 1555.
9. M. C. Etter, J. C. Macdonald, J. Bernstein, *Acta Crystallogr. B* **1990**, *46*, 256.
10. M. C. Etter, *Acc. Chem. Res.* **1990**, *23*, 120.
11. N. Jaiboon, K. Yos-In, S. Ruangchaitaweek, N. Chaichit, R. Thutivoranath, K. Siritaedmukul, S. Hannongbua, *Anal. Sci.* **2001**, *17*, 1465.
12. A. Nasirullah, N. U. Islam, M. N. Tahir, I. Khan, *Acta Cryst* **2011**, *E67*, o273.
13. M. J. Frisch, G. W. Trucks, H. B. Schlegel, G. E. Scuseria, M. A. Robb, J. R. Cheeseman, G. Scalmani, V. Barone, B. Mennucci, G. A. Petersson, H. Nakatsuji, M. Caricato, X. Li, H. P. Hratchian, A. F. Izmaylov, J. Bloino, G. Zheng, J. L. Sonnenberg, M. Hada, M. Ehara, K. Toyota, R. Fukuda, J. Hasegawa, M. Ishida, T. Nakajima, Y. Honda, O. Kitao, H. Nakai, T. Vreven, J. A. Montgomery Jr., J. E. Peralta, F. Ogliaro, M. Bearpark, J. J. Heyd, E. Brothers, K. N. Kudin, V. N. Staroverov, R. Kobayashi, J. Normand, K. Raghavachari, A. Rendell, J. C. Burant, S. S. Iyengar, J. Tomasi, M. Cossi, N. Rega, N. J. Millam, M. Klene, J. E. Knox, J. B. Cross, V. Bakken, C. Adamo, J. Jaramillo, R. Gomperts, R. E. Stratmann, O. Yazyev, A. J. Austin, R. Cammi, C. Pomelli, J. W. Ochterski, R. L. Martin, K. Morokuma, V. G. Zakrzewski, G. A. Voth, P. Salvador, J. J. Dannenberg, S. Dapprich, A. D. Daniels, O. Farkas, J. B. Foresman, J. V. Ortiz, J. Cioslowski, D. J. Fox, *Gaussian 09, Revision A. 02*, Gaussian, Inc, Wallingford, CT, **2009**.
14. F. L. Hirshfeld, *Theoretica Chimica Acta* **1977**, *44*, 129.
15. M. A. Spackman, D. Jayatilaka, *CrystEngComm* **2009**, *11*, 19.
16. S. K. Wolff, D. J. Grimwood, J. J. McKinnon, M. J. Turner, D. Jayatilaka, M. A. Spackman, *University of Western Australia*, **2012**.
17. S. Long, P. Zhou, K. L. Theiss, M. A. Siegler, T. Li, *CrystEngComm* **2015**, *17*, 5195.
18. S. Long, P. Zhou, S. Parkin, T. Li, *CrystEngComm* **2015**, *17*, 2389.
19. G. M. Sheldrick, *University of Gottingen*, **1997**.
20. G. M. Sheldrick, *Acta Cryst* **2008**, *A64*, 112.
21. S. Long, M. Zhang, P. Zhou, F. Yu, S. Parkin, T. Li, *Crystal Growth and Design* **2016**, *16*, 2573.